ORIGINAL PAPER

Atrophy of submandibular gland by the duct ligation and a blockade of SP receptor in rats

Sumiyo Hishida[1,5], Noriyuki Ozaki[2], Takashi Honda[3], Toshio Shigetomi[4], Minoru Ueda[5], Hideharu Hibi[5] and Yasuo Sugiura[6]

[1]*Department of Oral and Maxillofacial Surgery, National Hospital Organization Nagoya Medical Center, Nagoya, Japan*
[2]*Department of Functional Anatomy, Institute of Medical, Pharmaceutical and Health Science, Kanazawa University,Kanazawa, Japan*
[3]*Department of Human Life Sciences, Fukushima Medical University, School of Nursing, Fukushima, Japan*
[4]*Department of Oral and Maxillofacial Surgery, Nagoya Tokushukai General Hospital, Kasugai, Japan*
[5]*Department of Oral and Maxillofacial Surgery, Nagoya University Graduate School of Medicine, Nagoya, Japan*
[6]*Department of Child Care Studies, School of Human Care Studies, Nagoya University of Arts and Science, Nissin, Japan*

ABSTRACT

To clarify the mechanisms underlying the submandibular gland atrophies associated with ptyalolithiasis, morphological changes were examined in the rat submandibular gland following either surgical intervention of the duct or functional blockade at substance P receptors (SPRs). Progressive acinar atrophy was observed after duct ligation or avulsion of periductal tissues. This suggested that damage to periductal tissue involving nerve fibers might contribute to ligation-associated acinar atrophy. Immunohistochemically labeled-substance P positive nerve fibers (SPFs) coursed in parallel with the main duct and were distributed around the interlobular, striated, granular and intercalated duct, and glandular acini. Strong SPR immunoreactivity was observed in the duct. Injection into the submandibular gland of a SPR antagonist induced marked acinar atrophy. The results revealed that disturbance of SPFs and SPRs might be involved in the atrophy of the submandibular gland associated with ptyalolithiasis.

Key Words: duct ligation, atrophy, nerve fiber, submandibular gland, substance P receptor

INTRODUCTION

Submandibular gland atrophy is a serious condition that is often associated with ptyalolithiasis. Various investigators have sought to identify the basis of this atrophy. A duct ligation model is often used, since ligation can induce atrophy of glandular cells.[1-3] Many experiments involving salivary duct ligation in small animals have interpreted their results as showing that an increase in pressure within the gland caused by duct ligation acts as a physical stimulus upon acinar epithelial cells to induce atrophy.[4-9] In these reports, however, duct ligation induced atrophy

---

mainly in acinar cells, while duct epithelial cells remained intact regardless of the dilation of the lumen. Had increased intraductal pressure been the cause of atrophy, both acinar cells and ductal epithelial cells should have been affected. In addition to an increase in pressure within the gland, other factors therefore should be considered as contributors to atrophy of acinar cells in duct ligation models.

Atrophy of salivary glands in fact can be induced even without duct obstruction, such as by parasympathetic or sympathetic denervation.[10] These findings suggest that peripheral innervation has an important trophic function in maintaining the submandibular gland, and this raises the question of whether denervation might be involved in submandibular atrophy in duct ligation models.

Previous studies[3, 11-13] reported that parasympathetic nerves in the rat submandibular gland follow the course of the submandibular duct from the chordalingual nerves. They enter periductal ganglia, which give rise to fine, branching fibers that penetrate the glandular body. In addition to increasing pressure within the duct, ligation of the submandibular duct injures nerves passing through periductal tissues, which might also affect acinar cells. We therefore readdressed the question of the mechanisms of salivary gland atrophy in the ligation model.

We devised two different models in addition to the ligation model. In one group of rats, only the nerves surrounding a spared salivary duct were damaged. In another, the pressure within the duct was elevated by obstruction of the orifice, without nerve injury. We compared subsequent morphological changes in the submandibular gland. We then focused on Substance P (SP) and its receptor SPr, localized them immunohistochemically and determined whether a locally injected SP antagonist could induce atrophy in the gland.

MATERIALS AND METHODS

Experimental animals

Fifty-four 12-week-old male Wistar rats were used in the experiments. The rats had free access to water and standard feed, and were kept in a room with a light-dark cycle (12:12 h) and a controlled temperature (23°C).

Animal surgery

Rats were anesthetized with sodium pentobarbital (Nembutal, Abbot Laboratories, Chicago, IL, USA; 50 mg/kg i.p.). A midline ventral cervical skin incision about 20 mm long was made under sterile conditions. We isolated the main ducts of the submandibular gland from accompanying blood vessels and nerves on both sides using a surgical microscope. In the first group, the ducts were ligated with 3–0 silk sutures at the midportion of the duct (duct ligation group: DL group). In the second group, the ducts were carefully isolated from surrounding connective tissues (periductal avulsion group: PA group). In the third group, the orifice of the duct was ligated with 8–0 silk sutures at the caruncula sublingualis in the oral cavity (duct obstruction group: DO group). In a fourth group including three rats, submandibular glands were injected with 5 μl of Spantide III (BIOMOL International, L.P., Plymouth Meeting, PA, USA) as a SP antagonist.

This study was conducted with the approval of the local animal ethics committee in accordance with the Regulations for Animal Experiments in Nagoya University and the Animal Protection and Management Law of the Japanese Government (No. 105).

Tissue specimens

Three rats in each of the three surgical groups were killed at 1, 3, 5 and 7 days after surgery.

As a control, submandibular glands were taken from rats without surgery according to the same schedule. The three rats injected with Spantide III were killed 3 days following injection. They were anesthetized with pentobarbital sodium (Nembutal, 50 mg/kg i.p.), and perfused transcardially with 300 ml of heparinized saline, followed by the same volume of 4% paraformaldehyde (PFA) in 0.1 M phosphate buffered saline (PBS). After perfusion, submandibular glands were removed bilaterally and postfixed with PFA for 10 h at 4°C. Then, the submandibular glands were cut in half along the plane parallel to the main duct. One half was used for histopathological examination, and the other for immunohistochemical staining.

Histological analysis

Tissue samples were embedded in paraffin after dehydration through a graded alcohol series, and then cut into 3 μm sections on a microtome. Sections were mounted on slides coated with albumin adhesive. The paraffin sections were stained with hematoxylin and eosin (H-E) for general morphology. The Periodic acid Schiff (PAS) - Alcian blue (AB) method was used for the demonstration of acinar and ductal secretary granules.[14]

Measurement of cell and nuclear size

In tissue sections of the submandibular gland 3 days after surgery, we measured the major axes of acinar cells and of their nuclei (n=100), using a light microscope at 400x magnification equipped with a computer-aided microscopic image analyzing system (Neurolucida; Microbrightfield, Colchester, VT, USA). Data obtained from the control group, DO group, DA group, and DL group were compared. Statistical analysis was conducted by one-way analyses of variance (ANOVA), while significance was determined using the Kruskal Wallis test.

Tissue preparation for immunohistochemistry

Tissues were immersed in 20% sucrose solution for cryoprotection overnight at 4°C and then embedded in an optimal cutting temperature compound (Tissue-Tek, Sakura, Tokyo, Japan) and frozen rapidly at –80°C. Two sets of 15 μm serial sections were cut on a cryostat. Sections were mounted on slides coated with chrome-alum and gelatin, and dried at room temperature.

*Immunohistochemistry of SP and SPr in the submandibular gland*

After rinsing with 0.1 M PBS, a set of sections was allowed to react with polyclonal rabbit anti-SP antibody (Biogenesis, London, UK) at a dilution of 1:2000 in PBS containing 4% normal goat serum (Vector Laboratories, CA USA) for 2 h at room temperature. The other set of sections was incubated with 1 μg/ml affinity-purified polyclonal rabbit antibody against the SPr in PBS containing 2% normal goat serum for 48 h at 4°C.[15] The specificity of this antibody against SPr has previously been checked using the immunoblotting test.[16]

The activity of endogenous peroxidase in tissues was quenched by immersing sections in methyl alcohol containing 0.03% hydrogen peroxide for 30 min. After rinsing with PBS, sections were reacted with biotinylated goat anti-rabbit IgG (Vector Laboratories) at a dilution of 1: 200 in 0.1 M PBS for 2 h at room temperature. Next, sections were allowed to react with avidin-biotin-peroxidase complex (Vector Laboratories) at a dilution of 1:100 in 0.1 M PBS for 90 min. SP was visualized by peroxidase enzyme histochemistry using 0.1% 3,3' diaminobenzidine tetrahydrochloride (DAB; Sigma, St Louis, MO, USA) as a chromogen. Sections were counterstained with an aqueous solution of 1% methyl green prior to coverslipping.

Sumiyo Hishida *et al.*

RESULTS

Histological features of normal submandibular gland

Figure 1 shows the structure of a submandibular gland of a naïve rat stained using the PAS-AB method. The submandibular gland is a tubuloacinar gland composed of acini and intercalated, granular, and striated ducts. In the secretory portion, serous acini represent a major component and have a cuboidal epithelium that is strongly AB-positive (arrowheads). On the other hand, the intercalated duct shows reduced AB staining but is PAS-positive (arrows). Granules in granular duct cells are PAS-positive (large arrows). All striated ducts are PAS-positive and AB-negative. Each secretory unit is sheathed with loose interstitial connective tissue forming small lobules.
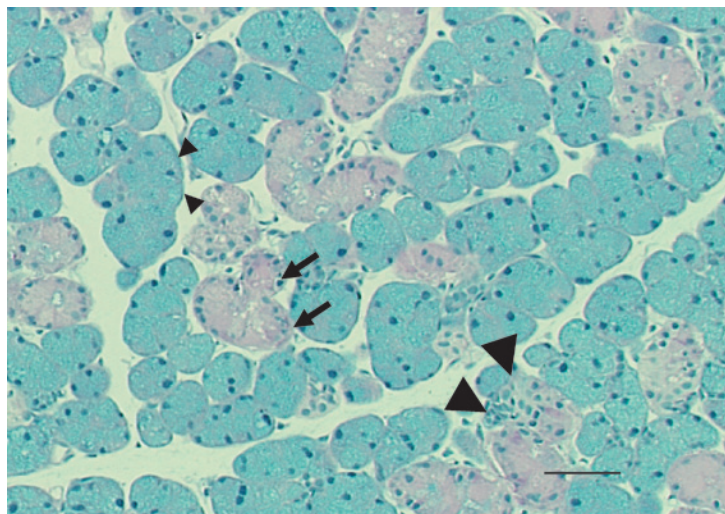
Fig. 1 Histological structure of the submandibular gland in a control rat (PAS-Alcian blue staining, bar:100 µm). Cells of the simple cuboidal epithelium of acini form secretory granules and are stained strongly by Alcian blue. Alcian blue staining is decreased in the intercalated duct, which is PAS-positive (large arrow). The striated duct was entirely PAS-positive and Alcian blue-negative (arrows). Small arrowheads indicate the epithelial cells of acini.

Histological changes after surgical manipulations of the ducts

1. Duct ligation (DL) group (Fig. 2a, b, c,)

Atrophy of acini epithelial cells and dilation of ducts were observed 1 day after ligation. These changes progressed rapidly over time. After 3 days, marked atrophy and degeneration of epithelial cells (2a, arrowheads) were seen in all lobules, precluding histological discernment of individual acini. Almost all ducts were greatly dilated and contained amorphous materials in the lumen (2a, arrows). Some of the remaining acini cells and duct cells had condensed nuclei, which have been identified as apoptotic changes. Infiltration by inflammatory cells was evident. On day 5 scattered acini (2b, arrowhead) could be seen in the lobules. Dilated duct-like structures with the proliferation of ductal cells (2b, arrows) were apparent. At 7 days postoperatively most acinar cells had disappeared. The number of duct-like structures had increased, and some of them were extremely dilated (2c, arrows). Infiltration by inflammatory cells still existed.

2. Duct obstruction (DO) group (Fig. 2d, e, f)

One day after duct obstruction, the epithelial cells of acini showed slight atrophic changes. In the duct, epithelial cells were flattened and the lumen was slightly expanded. Interlobular spaces were widened, implying the presence of edema.

At 3 days after obstruction, the epithelial cells of acini showed progressive atrophy (Fig. 2d, arrowhead). Duct dilation (2d, arrows) and an edematous appearance persisted at this stage.

After 5 days, the epithelial cells of acini showed even greater atrophy (Fig. 2e, arrowheads) and infiltration by inflammatory cells was present. Continued dilation of ducts was apparent.

At day 7, despite duct dilation (Fig. 2f, arrows), acini (arrowhead) had recovered their normal morphological features (Fig. 2f) as seen in naïve control animals.

3. Periductal avulsion (PA) group (Fig. 2g, h, i)

On the first day of PA, atrophy of epithelial cells in acini was found, and the size of acini in lobules was irregular. Slight dilation of the ducts was observed. Infiltration by inflammatory cells was present. Three days after PA, atrophy of epithelial cells was seen in all acini (Fig.
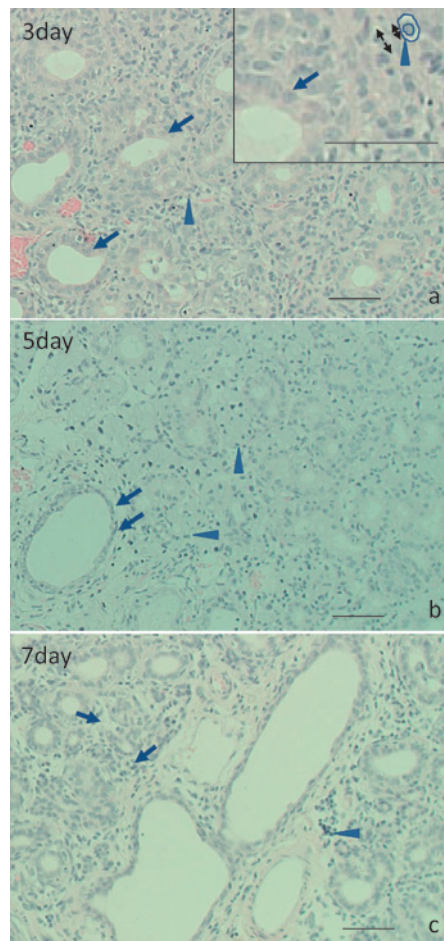
Fig. 2 duct ligation group (DL group)

Sumiyo Hishida *et al.*
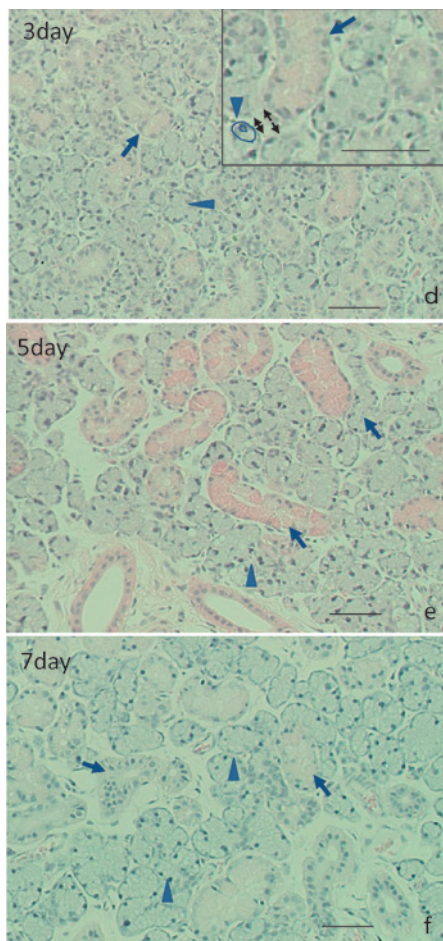
Fig. 2 duct obstruction group (DO group)

2g, arrowhead), and the interlobular space was increased, implying the presence of edema. At day 5, epithelial cells in acini showed advanced atrophic features (2h, arrowhead), but ducts only showed moderate dilation of the lumen (2h, arrows). At day 7, atrophy of acini cells (2i, arrowheads) and ductal cells (2i, arrows) had progressed and interstitial spaces had grown larger, reflecting edema.
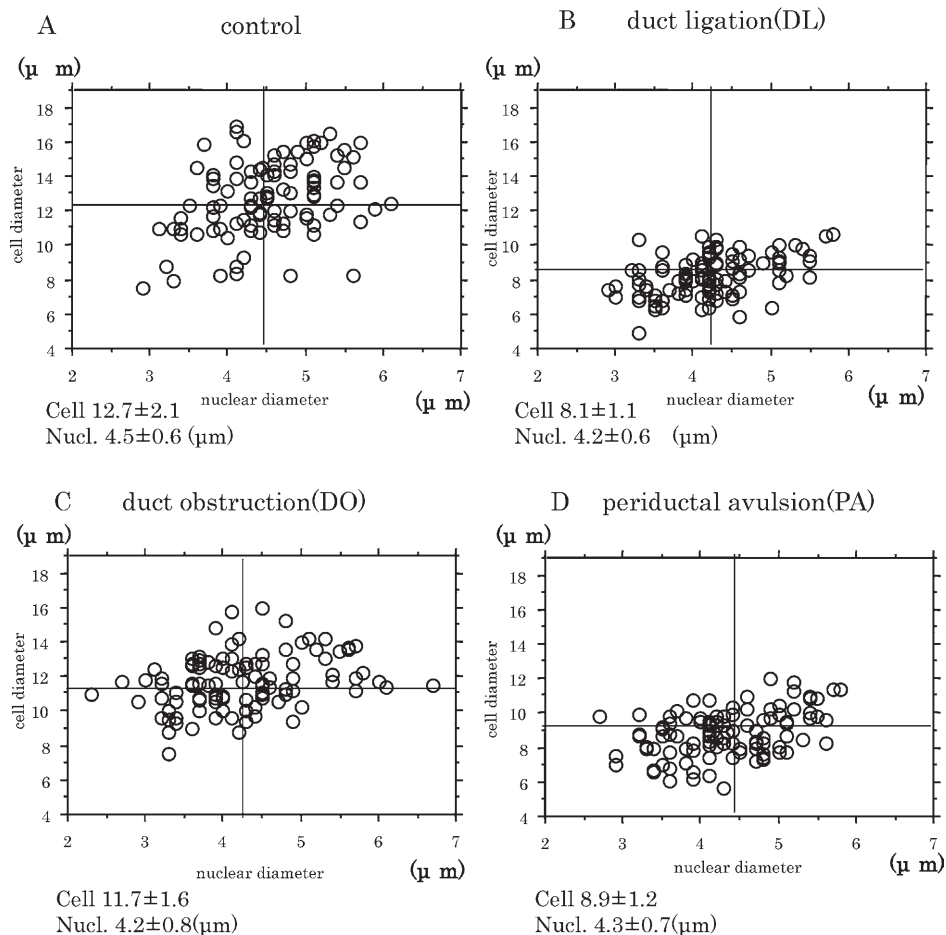
Comparison of acinar epithelial cell sizes

We measured the long axis of cell bodies and the nuclei of acinar epithelial cells 3 days after surgical manipulation. Figure 3 shows the mean sizes of cell and nuclear parameters. Differences in cell size were significant between naïve control (12.7±2.1 μm) and DL groups (8.1±1.1 μm) and between naïve control and PA groups (8.9±1.1 μm) (p<0.05). No significant difference in cell size was found between control and DO groups. No difference in the nuclear size of acinar epithelial cells was found between controls, and DL or DO groups.

Substance P for the submandibular gland
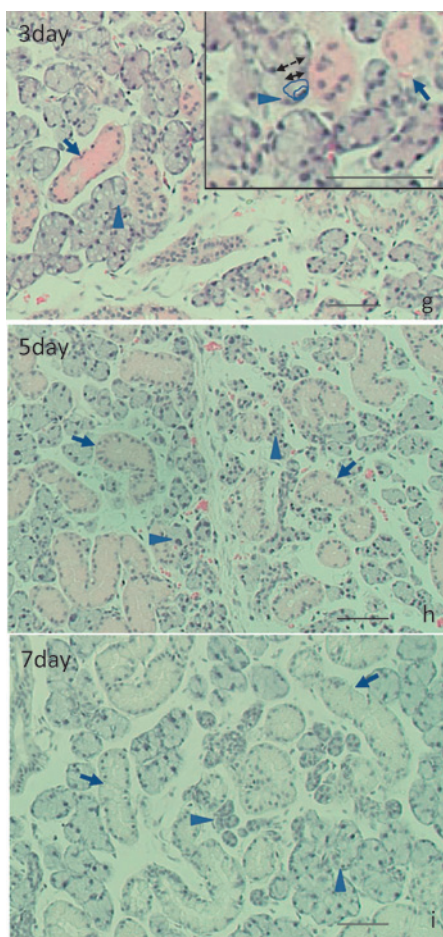
Fig. 2 periductal avulsion group (PA group)

Fig. 2 Histological changes in submandibular glands in experimental groups (PAS-Alcian blue staining, bar: 100 μm). a, b, c, : 3, 5 and 7 days after duct ligation (DL), respectively. d, e, f : 3, 5 and 7 days after duct obstruction (DO), respectively. g, h, i : 3, 5 and 7 days after periductal avulsion (PA). Insets in a,d,g are high magnification of each picture showing cell and nuclear measurement(dot line arrowed solid line arrowed)

2a: Atrophic epithelial cell features of acini (arrowheads) and dilation of intercalated and striated ducts (arrows) were observed after 3 days of DL. 2h: Marked atrophy and degeneration of epithelial cells were seen in all lobules, and almost all ducts were greatly dilated. Epithelial cells in the intercalated ducts showed mitoses, and scattered acini (arrowhead) could be seen in lobules despite the dilation of ducts (arrow) at 5 days after DL. 2c: At 7 days after DL, epithelial cells of acini had disappeared, while all ducts were extremely dilated (arrows). 2d: Epithelial cells of acini showed slight atrophy (arrowheads). Epithelial cells of the ducts were flattened and the lumens expanded (arrows) after 3 days of duct obstruction (DO). 2e: After 5 days DO, epithelial cells of acini had recovered morphologically (arrowheads) and ducts were slightly dilated. 2f: At 7 days after DO, epithelial cells of acini had recovered normal morphological features despite edematous tissue. 2g: Periductal avulsion (PA) caused the atrophy of epithelial cells in acini and the size of acini in lobules to be irregular. 2h: Atrophic and vacuolized epithelial cell features of acini (arrowheads) were observed after 3 days of PA. 2h: At 5 days after PA, epithelial cells of acini showed atrophic features (arrowhead), but ducts showed less change (arrow) and the interlobular space was dilated. 2i: At 7 days after PA, atrophy of acini had progressed (arrowhead), and spaces had grown larger, reflecting edema around ducts (arrows).

222

Sumiyo Hishida *et al.*

A   control

B   duct ligation(DL)

C   duct obstruction(DO)

D   periductal avulsion(PA)

Cell 12.7±2.1
Nucl. 4.5±0.6 (μm)

Cell 8.1±1.1
Nucl. 4.2±0.6　(μm)

Cell 11.7±1.6
Nucl. 4.2±0.8(μm)

Cell 8.9±1.2
Nucl. 4.3±0.7(μm)

Fig. 3 Comparison of acinar epithelial cell and nuclear sizes between groups. Acinar cell and nuclear diameters in submandibular gland are indicated in X and Y-axis respectively. Data are expressed as mean ± SEM. Cell sizes in the PA and DL groups were significantly smaller than in the control. Nuclear size was reduced in the DO and DL group compared to the control. Cell and Nucl indicate the mean diameter of cell and nuclear size.
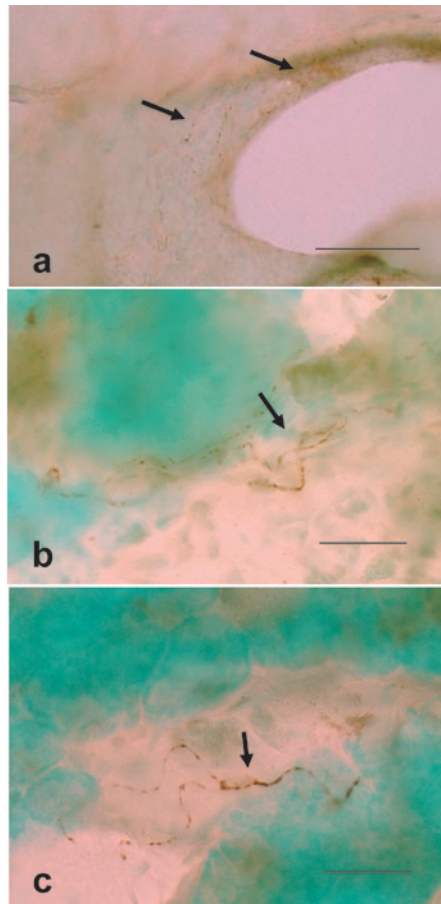
SP-positive nerve fibers in the submandibular gland

The fine SP-positive nerve fibers formed a network on the external surface of the main duct that penetrated the secretory units of the submandibular gland. These fine SP-positive fibers branched into the lobules of the gland along the lobular duct (Fig. 4a). Along the lobular duct, fine fibers coursed around the external surface of the duct and branched repeatedly to single fibers, terminating with many fiber swelling or beaded forms. These terminals were distributed on the surface of the ducts (Fig. 4b, 4c), but not around acinar secretory cells.

Distribution of SPr-positive cells

SPr-positive cells were observed in the ducts (Fig. 5a, 5b arrows). SPr reactivity was present in the cytoplasm but not in the nucleus. No SPr-positive cells were observed in acini.

Fig. 4 Substance P (SP) positive nerve fibers (arrows) in submandibular gland (bar: 100 μm). SP-positive nerve fibers (arrows) are abundant within the body of the submandibular gland and form a reticular pattern along the outer wall of the main duct. a: SP-positive nerve fibers along the main duct of the submandibular gland (SMD), passing to the intralobular duct. b: Distribution of SP-positive nerve fibers along an intralobular duct. c: Distribution of SP-positive nerve fibers from the intercalated duct to the striated duct.

Effect of SPr antagonist on the submandibular gland

Figure 6 shows the submandibular gland 3 days following local injection of saline (a) or Spantide III (b). Although the saline-injected submandibular gland showed a normal histological structure as in control submandibular glands (Fig. 6a), the acini at the antagonist injection site had degenerated completely and disappeared (Fig. 6b). The cells remaining in the degenerated lobules were PAS-positive and AB-negative, and appeared similar to epithelial cells of intercalated and striated ducts (Fig. 6b). Marked pathological changes were restricted to the secretory acinar portion (surrounded by arrows), sparing the ducts. Infiltrating lymphocytes and occasional neutrophils were observed in the lobules.

Sumiyo Hishida *et al.*
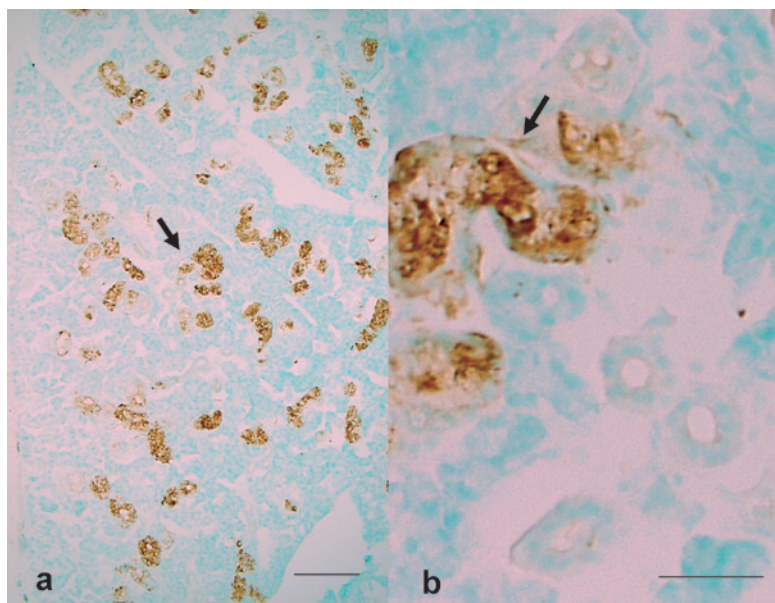
Fig. 5 Distribution of SPr-positive cells (arrows) in submandibular gland. a: Low magnification picture of submandibular gland, SPr-positive cells are restrictedly expressed in epithelial cells of the duct (bar: 100 μm). b: Higher magnification of the duct cells, which shows strongly immunopositive deposits and striated ducts and intercalated ducts are continuedly.
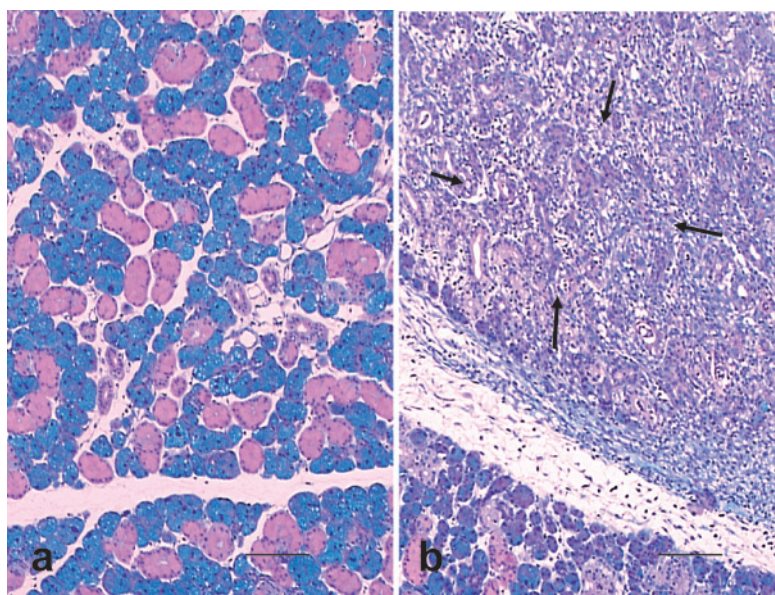
Fig. 6 Influence of a substance P-receptor antagonist on submandibular gland morphology (bar: 100 μm). a: Submandibular gland injected with saline. The submandibular gland showed completely normal features. b: Submandibular gland injected with substance P-receptor antagonist. Upper side of this submandibular gland was completely atrophied and degenerated (surrounded by arrows). Some ducts appeared in the degenerated submandibular gland, but no acinar cells were found except in small numbers at the margin of the capsules.

DISCUSSION

Mechanisms causing atrophy of the submandibular gland

The salivary gland frequently atrophies following ptyalolithiasis, sialadenitis, salivary gland tumors, Sjogren's syndrome or salivary gland surgery. Such atrophy seriously affects salivary secretion.[17-20]

Changes in the submandibular gland associated with duct ligation in the present study are consistent with the results of earlier studies.[1,21,22] In brief, degeneration and disappearance of acinar cells occurred at an early stage after duct ligation, while epithelial cells in the duct remained histologically less affected. Five days after duct ligation, a small number of immature acinar epithelial cells could be seen. However by 7 days after duct ligation, regenerated acinar cells had atrophied and degenerated. Our observations enabled the division of events in the submandibular gland after duct ligation into an acute degenerative/regenerative phase and a chronic degenerative phase. It has previously been reported that at 2 and 3 days after duct ligation, increased numbers of PCNA (a marker of proliferating cells) positive cells were seen in ducts but thereafter PCNA positive cells decreased in number.[25] Epithelial cells of the intercalated duct have been reported to be potential reserve cells for repopulating acini.[21,23,24] A short-lived cycle of duct cell proliferation may take place during the acute degenerative/regenerative phase after duct ligation.

Submandibular glands following orifice ligation showed changes differing from that following duct ligation. In the earlier stage of both manipulations, dilation of the lobular duct lumen was found, and intraductal pressure likely would have been increased. In this acute stage, degeneration and regeneration were found in the acinar cells after either duct or orifice ligation. However, the chronic stage differed between models. Acinar cells eventually disappeared after duct ligation, while in rats with orifice obstruction these cells were preserved in the chronic phase. The chorda lingual (CL) nerve, which is a branch of the lingual nerve, crosses the submandibular duct and carries parasympathetic fibers to the submandibular glands.[12] The nerve plays a major role in evoking the secretion of submandibular saliva, and also has a trophic effect on salivary glands.[26] Experimental obstruction of the main excretory ducts by orifice obstruction did not damage the CL nerve,[3] and therefore likely induced less severe atrophy of the gland compared to duct ligation.

Acinar atrophy was also present to a mild degree in rats with periductal avulsion. In these rats, the time courses of acinar atrophy clearly differed from findings in duct ligation and orifice obstruction experiments. While degeneration occurred rapidly in the acute stage after duct ligation, periductal avulsion resulted in gradual degeneration throughout the experiment. Acinar cells were not maintained and did not regenerate, showing prolonged derangement of the submandibular gland. Therefore, periductal tissue components presumably included some elements that promoted the maintenance and regeneration of acini.

Trophic functions of SP-positive nerve fibers and SPr in submandibular gland

As mentioned above, ongoing atrophy of acini associated with periductal avulsion continued even in the late phase, suggesting loss of trophic factors. These findings were similar to atrophy of the submandibular gland seen after sectioning of either parasympathetic or sympathetic nerve fibers.[9,26]

Many reports have described the innervation of the submandibular gland, including autonomic and somatosensory nervous systems.[27] An important role for parasympathetic fibers from the tympanic nerve in maintaining the submandibular gland has been suggested.[10] Previous studies reported that the lingual nerves supply parasympathetic fibers as they course in the vicinity of the main duct.[28] Postganglionic parasympathetic neurons innervating the submandibular gland

were located along the salivary ducts, and their axons formed a reticular pattern around the duct, then entered the gland.[11,13] In contrast to parasympathetic innervations, paraganglionic sympathetic nerves from the superior cervical ganglion usually enter glands along arteries and ramify with them.[3] In addition to efferent fibers, the sympathetic and parasympathetic nerve routes leading to the rat submandibular gland contain sensory nerves which mainly originate from the dorsal root ganglia and trigeminal ganglion, respectively.[29] Accordingly, parasympathetic efferent nerves are associated with sensory afferents but not sympathetic efferents.

In addition to the importance of innervation of the submandibular gland, the SPr is critical. The SPr is strongly expressed in epithelial cells in the ducts. Topical administration of an antagonist of SPr induced the degenerative atrophy and disappearance of acini. These findings indicate the importance of SP and its receptor SPr in maintaining the morphology and function of acini. Most neuropeptides including SP[30-32] act not only as transmitters between synapses in the spinal cord, but are also discharged from nerve endings to peripheral tissues, where they carry out physiological activities in response to various stimuli.[33] These peptides appear to have functional and trophic activity in the submandibular gland.

In the present study we could not identify the origin of SP-positive fibers in the submandibular gland. Immunohistochemical study combined with denervation suggested that postganglionic parasympathetic nerves are the major source of substance P in the rat submandibular gland.[33] In addition, sensory nerves from the trigeminal ganglion are likely to be involved.[29]

In the absence of SPr on the acinar cells, it is interesting that the reduction in SP due to duct ligation or functional blockade of SPr by injection of an antagonist causes atrophy of the acini. As the turnover of acinar cells is normally relatively slow, mechanisms underlying the rapid atrophy after manipulation are not clear. The duct cells might have a trophic effect on the acinar cells, perhaps by secretion of a paracrine substance that is regulated by SP. Further studies are needed to clarify the situation.

We have shown that avulsion of periductal tissues surrounding a spared salivary duct induced acinar atrophy. Our immunohistochemical study revealed that SPr was localized in the duct. Finally injection of a SPr antagonist into the submandibular gland induced marked acinar atrophy. The results revealed that disturbance of SPFs and SPRs might be involved in the atrophy of the submandibular gland associated with ptyalolithiasis.

REFERENCES

1) Tamarin A. Submaxillary gland recovery from obstruction I. Overall changes and electron microscopic alterations of granular duct cells. *J Ultrastr Res*, 1971; 34: 276–287.

2) Harrison JD, Fouad HM, Garrett JR. Variation in the response to ductal obstruction of feline submandibular and sublingual salivary glands and the importance of the innervation. *J Oral Pathol Med*, 2001; 30: 29–34.

3) Osailan SM, Proctor GB, McGurk M, Paterson K. Intraoral duct ligation without inclusion of the parasympathetic nerve supply induces rat submandibular gland atrophy. *Int J Exp Pathol*, 2006; 87: 41–48.

4) Bhaskar SN, Bolden TE, Weinmann JP. Experimental obstructive adenitis in the mouse. *J Dent R*, 1956; 35: 852–862.

5) Shiba R, Hamada T, Kawakatsu K. Histochemical and electron microscopical studies on the effect of duct ligation of rat salivary glands. *Arch Oral Biol*, 1972; 17: 290–309.

6) Harrison JD, Garrett JR. The effects of ductal ligation of the parenchyma of salivary glands of cat studied by enzyme histochemical methods. *Histochem J*, 1976; 8: 35–44.

7) Nilsson BO, Ekström J, Rosengren E. Polyamine metabolism in rat parotid gland after duct ligation. *Acta Physiol Scand*, 1987; 131: 177–181.

8) Norkerg LE, Abok K, Lundquist PG. Effects of ligation and irradiation on the submaxillary glands in rats.

Acta Otolaryngol, 1988; 105: 181–192.

9) Snell RS, Garrett JR. The effect of postganglionic sympathectomy on the structure of the submandibular and major sublingual salivary glands of the rat. *Z Zellforsch*, 1958; 48 :639–652.

10) Kyriacou K, Garrett JR. Morphological changes in the rabbit submandibular gland after parasympathetic or sympathetic denervation. *Arch Oral Biol*, 1988; 33: 4: 281–290.

11) Lichtman JW. The reorganization of synaptic connections in the rat submandibular ganglion during post-natal development. *J Physiol*, 1977; 273: 155–177.

12) Kawa K, Roper S. On the two subdivisions and intrinsic synaptic connections in the submandibular ganglion of the rat. *J Physiol*, 1984; 346: 301–320.

13) Tsuboi T, Honda T, Hishida S, Shigetomi T, Ueda, M, Sugiura Y. A quantitative study of nerve fiber density in the submandibular gland of rats. *Nagoya J Med Sci*, 2004; 67: 25–34.

14) Carpenter GH. Altered plasticity of the parasympathetic innervations in the recovering rat submandibular gland following extensive atrophy. *Exp Physiol*, 2009; 94: 213–219.

15) Honda T, Ozaki T, Tonosaki Y, Nishiyama K, Shigemoto R, Sugiura Y. Synaptic organization and ultra-structural features of the substance P-receptor-like immunoreactive neurons in the nucleus intermediolateralis of rats. *Neurosci Lett*, 1995; 197: 117–120.

16) Shigemoto R, Nakaya Y, Nomura S, Ogawa-Meguro R, Ohishi H, Kaneko T, *et al.* Immunocytochemical localization of rat substance P receptor in the striatum. *Ncurosci Lett*, 1993; 153: 157–160.

17) Tandler B. Ultrastructure of chronically inflamed human submandibular glands. *Arch Pathol Lab Med*, 1977; 101: 425–431.

18) Grisius MM. Salivary gland dysfunction: A review of systemic therapies. *Oral Surg Oral Med Oral Pathol Oral Radiol Endod*, 2001; 92: 156–162.

19) Daniels TE, Wu AJ, Calif J. Xerostomia-clinical evaluation and treatment in general practice. *Dent Asso*, 2001; 28: 933–941.

20) Taylor SE, Miller EG. Preemptive pharmacologic intervention in radiation-induced salivary dysfunction. *Proc Soc Exper Biol Med*, 1999; 221: 14–26.

21) Takai Y, Asano K, Clemente RP, Mori M. Lectin histochemistry of submandibular glands following duct-ligation in mice and rats. *J Oral Pathol*, 1985; 14: 740–749.

22) Tamarin A. Submaxillary gland recovery from obstruction. Electron microscopic alterations of acinar cells. *J Ultrastructure Research*, 1971; 34: 288–302.

23) Hanks CT, Chaudhry A. Regeneration of rat submandibular gland following partial extirpation; A light and electron microscopic study. *Am J Anat*, 1971; 130: 195–207.

24) Hecht R, Connelly M, Marchetti L, Ball WD, Hand AR. Cell death during development of intercalated ducts in the rat submandibular gland. *Anat Rec*, 2000; 258: 349–358.

25) Takahashi S, Nakamura S, Suzuki R, Islam N, Domon T, Yamamoto T, *et al.* Apoptosis and mitosis of parenchymal cells in the duct-ligated rat submandibular gland. *Tissue & Cell*, 2000; 32: 457–463.

26) Carpenter GH, Proctor GB, Garrett JR. Preganglionic parasympathectomy decreases salivary SIgA secretion rates from the rat submandibular gland. *J Neuroimmunology*, 2005; 160: 4–11.

27) Kobayashi M, Ichikawa H, Kobashi M, Funahashi M, Mitoh Y, Matsuo R. The origin of sensory nerve fibers that innervate the submandibular salivary gland in the rat. *Brain Res*, 2005; 1060: 184–187.

28) Proctor GB, Carpenter GH. Regulation of salivary gland function by autonomic nerves. *Auton Neurosci*, 2007; 133: 3–18.

29) Goedert M, Nagy JI, Emson.PC. The origin of substance P in the rat submandibular gland and its major duct. *Brain Res*, 1982; 252: 327–333.

30) Pernow B. Substance P. *Pharmacol Rev*, 1983; 35: 85–141.

31) Hökfelt T, Kellerth JO, Nilsson G, Pernow B. Experimental immunohistochemical studies on the localization and distribution of substance P in cat primary sensory neurons. *Brain Res*, 1975; 100: 235–252.

32) Takahashi T, Otsuka M. Regional distribution of substance P in the spinal cord and nerve roots of the cat and the effect of dorsal root section. *Brain Res*, 1975; 87: 1–11.

33) Ekström J, Brodin E, Ekman R, Hakanson R, Sundler F. Vasoactive intestinal peptide and substance P in salivary glands of the rat following denervation or duct ligation. *Regulatory Peptide*, 1984; 10: 1–10.